A Study on the Ability of Different Non-Intrusive Sensors for Diagnosing Outdoor Insulator Defects

Celal Fadil Kumru*[1,2], Abdulla Lutfi[1], Ayman El-Hag[1], Ahmad Darwish[3], Shady S. Refaat[4], Haitham Abu-Rub[4]
[1]*Department of Electrical and Computer Engineering*
University of Waterloo,
Waterloo, Canada
[2]*Department of Electrical and Electronics Engineering*
Suleyman Demirel University
Isparta, Türkiye
[3]*Department of Electrical Engineering*
Purdue University
Indiana, USA
[4]*Department of Electrical Engineering*
Texas A&M University
Doha, Qatar
*Corresponding author: celalkumru@sdu.edu.tr

2023 IEEE Electrical Insulation Conference (EIC) | 978-1-6654-9341-3/23/$31.00 ©2023 IEEE | DOI: 10.1109/EIC55835.2023.10177298

***Abstract*—Insulators' failures caused by any type of defect may result in serious technical and economic losses. In particular, contamination flashovers due to excessive pollution and humidity are one of the main problems encountered in power systems. Moreover, other types of defects like surface crack and internal void are other common examples of outdoor insulator defects that may lead to insulator failure. In this regard, detecting the defect using a non-intrusive method is important in terms of energy continuity and monitoring efficiency. Both vision (regular, IR and UV camera) and emission (RF, ultrasonic, and acoustic) based sensors have been deployed in the field to detect these defects. It has been reported that each sensor has certain pros and cons in terms of its ability to detect the different defects. Therefore, it is essential to investigate and compare the sensing performance of non-intrusive sensors for different defects. In this study, an ultrasonic sensor (20 - 100 kHz), an RF antenna (0.53 - 3 GHz) and an IR camera were used to detect dry band arcing, corona and surface discharge. All three sensors along with the standard partial discharge measurement system were used simultaneously for each measurement. The results show that sensing performance of the three sensors varies depending on the defect type.**

Keywords—outdoor insulation, insulator defects, acoustic sensor, RF antenna, IR camera

I. Introduction

Outdoor insulators are crucial components of power systems primarily due to their role in ensuring and maintaining system reliability. Despite accounting for only 5% of the overall cost of overhead lines, statistical data show that 70% of the power outages in the transmission systems and 50% of the total overhead line maintenance costs are caused by outdoor insulators [1].

Surface pollution and physical defects such as cracks, broken discs, corrosion, and internal voids are frequently encountered in outdoor insulators. Presence of these defect(s) may cause partial discharge (PD), leakage current (LC) and eventually flashover events in the insulator [2], [3]. Hence, it is important to inspect insulators to detect these defects at an early stage. Inspection of outdoor insulators using non-intrusive visual (regular, UV and IR camera) and emission based sensors (acoustic, ultrasonic and RF sensor) [3] has been widely used by both researchers and utilities. Given that different types of defects emit unique physical phenomena such as electromagnetic radiation, ultrasonic waves, and heat, a combination of one or multiple sensors can be utilized for effective defect detection. As a result, a significant number of recent studies have employed non-intrusive sensors to detect a diverse range of defects in outdoor insulators.

Among non-intrusive sensors, acoustic emission (AE) sensors are mostly preferred for detecting PD, corona, and surface discharges. Additionally, there are studies in which AE sensor is used to detect internal discharges on controlled samples [4]. RF antennas are also capable of detecting different types of defects like AE sensors. However, the frequency of electromagnetic waves emitted varies depending on the type of defect present [5]. Even the frequency of the wave emitted by a specific defect like an internal discharge varies according to the location, shape and dimensions of the defect. Apart from emission sensors, vision based sensors are also widely used, particularly in field applications [6]. Among these sensors, IR camera has been employed for monitoring the temperature of vital equipment. Moreover recently, it has been employed for outdoor insulation diagnostics. However, the defects that IR camera can detect are limited to defects that result in temperature increase. Therefore, it is essential to recognize the specific categories of defects that each sensor is capable of detecting.

In the literature, there is a shortage of research that compares the efficiency of these sensors to detect the same defect type. The objective of this study is to compare the sensing capability of AE sensor, RF antenna and IR camera for different defects like corona, surface discharge, dry band arcing (DBA). Simultaneous measurements were made on controlled samples using three non-intrusive sensors along with standard PD

measurement system. The results revealed that the sensors have varying capabilities in detecting identical defects. Additionally, employing several sensors can help in identifying the defect type.

II. Experimental Setup

The test setup given in Fig. 1 was used to generate controlled corona and surface discharge. While the inclined plane test (IPT) setup was used to generate DBA according to ASTM D2303 standard as depicted in Fig. 2. In both test setups, simultaneous measurements were made using ultrasonic sensor, RF antenna and IR camera. For all tested defects, the non-intrusive sensors are placed one meter away from the test samples.

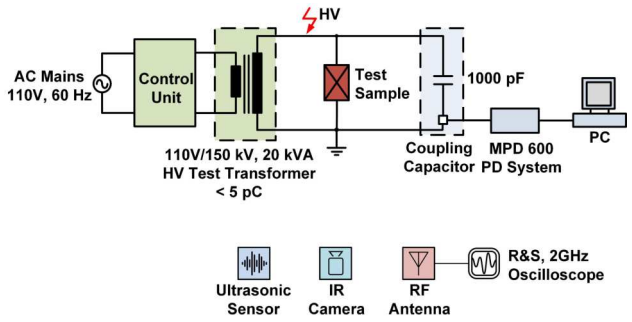

Fig. 1. Experimental setup for corona and surface discharge measurements

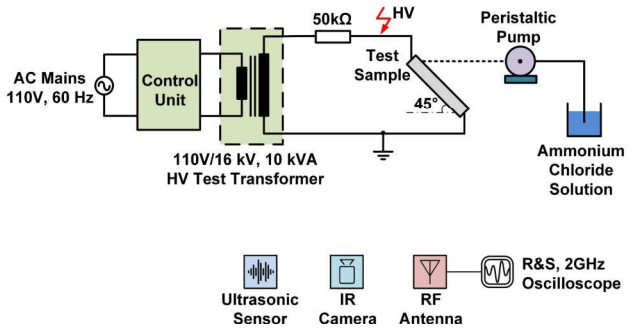

Fig. 2. IPT setup for DBA measurement

Before corona and surface discharge measurements, PD measurement system was calibrated at 10 pC charge. For PD measurements, center frequency and frequency bandwidth are set to 250 kHz and 300 kHz, respectively, in accordance with IEC 60270.

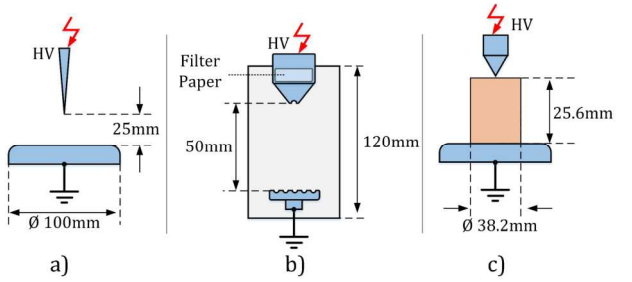

Fig. 3. Electrode and sample configurations for a) corona b) DBA c) surface discharge

Additionally, phase-resolved partial discharge (PRPD) patterns were recorded for a duration of one minute upon the initiation of sensor detection during the measurements of corona and surface discharge. Electrode configurations and samples given in Fig. 3 were used to simulate corona, DBA and surface discharge.

In Fig. 3a, a sharp point and plane electrode system with 25 mm air gap was used and the high voltage was applied to the sharp point and the plane electrode was grounded. As for the surface discharge, a cylindrical ceramic sample, as shown in Fig. 3c, is placed between the point-plane electrodes. In both measurements, voltage was gradually increased, and the sensor data were recorded after PD initiation. In DBA measurement, a polymer test sample (Fig. 3b) was used and 3.5 kV_{rms} AC test voltage was applied. The conductivity of the prepared contaminant solution was 2.6 mS/cm and the contamination flow rate was set to 0.6 ml/min. Sonotec-BS10 model ultrasonic sensor is used to measure AE signals, and the sensor can measure sound waves in the 20-100 kHz frequency band with 1 dB resolution. The RF antenna covers a frequency range between 0.5 GHz - 3 GHz with less than -10 dB reflection coefficient [7]. As for the heat sensing, FLIR T650 model IR camera that has ±1°C accuracy and NETD smaller than 20 mK is used. During the measurements, ambient conditions were monitored, and the mean values are given in Table 1.

TABLE I. Ambient Conditions During the Measurements

Temperature (°C)	Relative Humidity (%)	Pressure (mmHg)
22	16	730

III. Results and Discussion

In this section, data obtained from the three sensors for each defect is presented and their sensing performances are examined comparatively.

A. Corona

After the calibration of the PD system, the measurement of corona discharge commences through the application of a voltage of 2.5 kV. PD level at 2.5 kV voltage was smaller than 1 pC and the voltage is increased gradually with steps of 1 kV. For all test voltages below 13.8 kV, measured PD value was around 40 pC. At 13.8 kV, the measured PD increased to 5 nC and PRPD pattern produced is illustrated in Fig. 4. Both the ultrasonic sensor and RF antenna captured the corona signal only when the voltage reached 13.8kV (as depicted in Fig. 5). However, the IR camera could not detect any sign of corona discharge. This is because corona discharge is not intense enough to produce heat at the tip of the electrode.

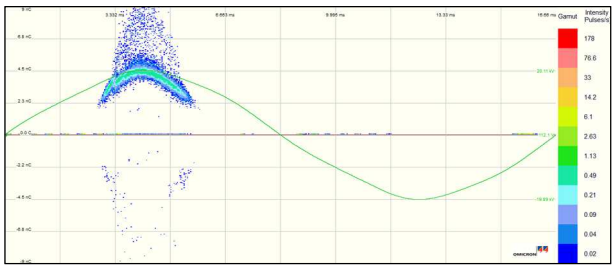

Fig. 4. PRPD pattern of corona at 13.8 kV

Even for longer durations like multiple days in the field, corona-induced heat can be effectively dissipated under external environmental conditions.

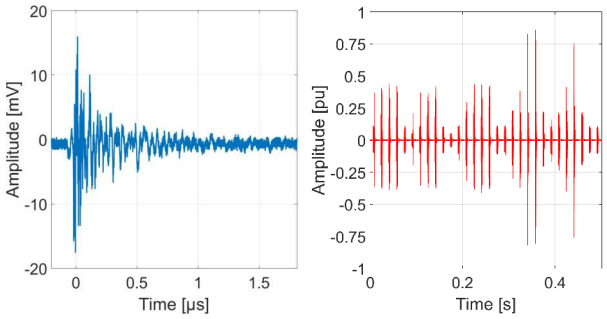

Fig. 5. Corona signals measured at 13.8 kV by a) RF antenna b) ultrasonic sensor

Therefore, it is not feasible to utilize an IR camera for corona detection due to its limitations. Consequently, when PD magnitude of a corona discharge reached a specific value, RF antenna and ultrasonic sensor were able to detect it. The magnitude of both acoustic and electromagnetic emissions depends on many factors such as sensor distance, intensity of discharge, path attenuation, noise, etc.

B. *Dry Band Arcing*

In DBA measurement, thermal images recorded with IR camera before and after the application of voltage are depicted in Fig. 6.

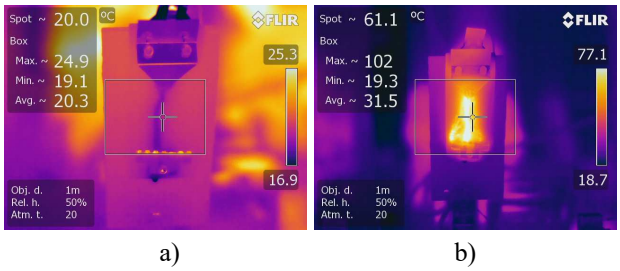

Fig. 6. Thermal images captured with IR camera a) before b) during DBA

In the presence of DBA, energy converted to heat due to low frequency arcs is higher than that of corona and surface discharges. Therefore, IR camera is able detect DBA as soon as it starts.

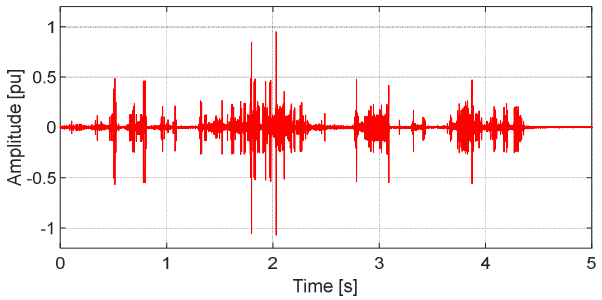

Fig. 7. DBA signal measured by ultrasonic sensor

In addition, as long as DBA continues, the heat generated by the arcs causes the polymer sample temperature to increase as seen in Fig. 6b. Moreover, ultrasonic sensor was successful in promptly detecting DBA signal as it initiated, and the resulting waveform is illustrated in Figure 7. One other hand, DBA emits low-frequency electromagnetic waves that are beyond the measuring range of the RF antenna [3]. Consequently, RF antenna was unable to capture DBA signal.

C. *Surface Discharge*

A typical PRPD pattern for the surface discharge is depicted in Fig. 8. Both the RF antenna and the ultrasonic sensor were capable of detecting surface discharges. However, the RF antenna captured the PD signal when PD magnitude reaches 90 pC at 2 kV and only when the applied voltage increased to 3 kV, the ultrasonic sensor detected PD signal at PD magnitude in the range of 500 pC. The waveforms of both captured signals are given in Fig. 9.

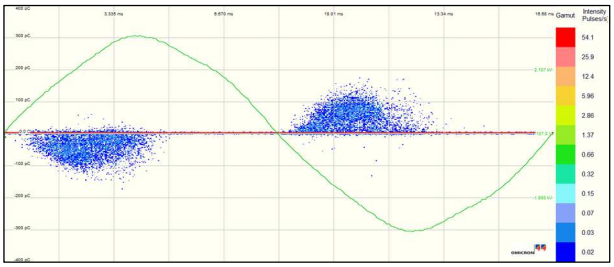

Fig. 8. PRPD pattern of surface discharge at 2 kV

The IR camera could not detect any temperature change at the PD levels used for the RF antenna or the ultrasonic sensor. Hence, in order to observe the heating effect of the surface discharges, 11 kV voltage was applied for two hours, and PD magnitude was around 4 nC. The thermal images of the test sample before and after the exposure to surface discharge for two hours are depicted in Fig. 10. It is evident that the temperature increased by around 1.2 °C.

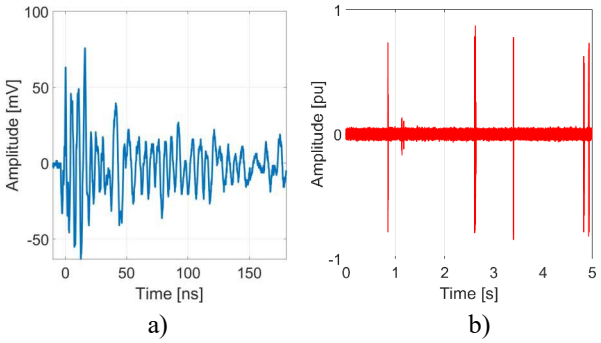

Fig. 9. Surface discharge signals measured by a) RF antenna at 2 kV b) ultrasonic sensor at 3 kV

Although the magnitude of PD observed during surface discharge was notably high at 11 kV, temperature increase was comparatively low. This is mainly because the heat generated from the surface discharge can be easily dissipated to the surrounding air by convection. Hence, surface discharges are

difficult to detect with an IR camera, especially in field conditions.

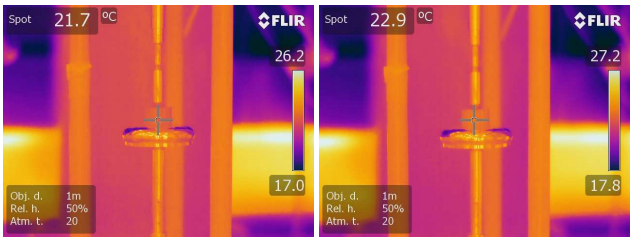

a) b)

Fig. 10. Thermal images captured with IR camera a) before test b) two hours after surface discharge

In Table 2, detection capability of the used sensors for different defect types are summarized. A single asterisk (*) indicates poor detecting performance, whereas a three-asterisks (***) rating signifies that the sensor is capable of capturing the related signal immediately upon PD activity initiation. A two-asterisks (**) rating indicates detection performance after PD activity has reached a certain level. Additionally, the dash symbol (-) indicates that the sensor is incapable of detecting a particular defect.

TABLE II. DEFECT BASED SENSING PERFORMANCES OF NON-INTRUSIVE SENSORS

Defect Types	**Non-Intrusive Sensors**		
	RF Antenna	***Ultrasonic Sensor***	***IR Camera***
Corona	**	**	-
Dry Band Arcing	-	***	***
Surface Discharge	***	**	*

Among these sensors, ultrasonic sensor was able to detect all types of defects indicated in the study. Hence, it can be stated that the ultrasonic sensor is a practical sensor mostly for detecting surface related defects. Moreover, the ultrasonic sensor is more cost effective than RF antenna that requires the use of expensive data acquisition system.

RF antenna was only able to detect corona and surface discharge. Despite the RF antenna employed in the study having a wide bandwidth, it was unable to detect the signal arising from DBA. This can be attributed to the low-frequency electromagnetic waves emitted by DBA that fall below the operating frequency band of the antenna. However, wet surface discharge due to the field enhancement at the triple point (water, air and insulator) may also be associated with high frequency electromagnetic wave and hence can be detected using RF antenna [8].

As for IR camera, while it showed a good sensing performance for detecting DBA, its ability to detect surface discharge is rather limited due to the relatively low temperature difference generated by surface discharge on the material surface. Therefore, it is even more difficult to detect small temperature differences with an IR camera in field conditions.

IV. CONCLUSION

This study involves the evaluation of sensing performances of three non-intrusive sensors for the detection of commonly encountered defects in outdoor insulators. Polymer samples were utilized as test specimens for DBA and ceramic sample was used for surface discharge measurements. All experiments were conducted when only one source of discharge is present at a time. Only ultrasonic sensor managed to detect all types of defects. Moreover, using multiple sensors can assist identifying the defect type. For example, when capturing a signal with the three non-intrusive sensors, this could be an indication of surface discharge on the insulator surface. However, if only RF antenna or ultrasonic sensor is used in the same case, signal waveform need to be further analyzed to specify the defect type. Therefore, using multiple sensors in the field applications may help identifying and classifying the defect type.

ACKNOWLEDGMENT

This study was granted by Scientific and Technological Research Council of Türkiye (TUBITAK) BIDEB 2219 and Natural Sciences and Engineering Research Council of Canada (NSERC) discovery grant no. RGPIN-2020-07004

REFERENCES

[1] S. Anjum, A. El-Hag, S. Jayaram, and A. Naderian, “Classification of defects in ceramic insulators using partial discharge signatures extracted from radio frequency (RF) signals,” *2014 IEEE Conf. Electr. Insul. Dielectr. Phenomena, CEIDP 2014*, pp. 212–215, 2014.

[2] A. Cavallini, S. Chandrasekar, G. C. Montanari, and F. Puletti, “Inferring ceramic insulator pollution by an innovative approach resorting to PD detection,” *IEEE Trans. Dielectr. Electr. Insul.*, vol. 14, no. 1, pp. 23–29, 2007.

[3] A. El-hag, “Application of Machine Learning Monitoring and Diagnostics,” *IEEE Instrum. Meas. Mag.*, vol. 24, no. 2, pp. 101–108, 2021.

[4] N. A. Al-Geelani, M. A. M. Piah, I. Saeh, N. A. Othman, F. L. Muhamedin, and N. F. Kasri, “Identification of acoustic signals of internal electric discharges on glass insulator under variable applied voltage,” *Int. J. Electr. Comput. Eng.*, vol. 6, no. 2, pp. 827–834, 2016.

[5] S. Anjum, S. Jayaram, A. El-Hag, and A. N. Jahromi, “Detection and classification of defects in ceramic insulators using RF antenna,” *IEEE Trans. Dielectr. Electr. Insul.*, vol. 24, no. 1, pp. 183–190, 2017.

[6] D. Pernebayeva, A. Irmanova, D. Sadykova, M. Bagheri, and A. James, “High voltage outdoor insulator surface condition evaluation using aerial insulator images,” *High Volt.*, vol. 4, no. 3, pp. 178–185, 2019.

[7] A. Darwish, S. S. Khalil, H. Abu-Rub, and H. Toliyat, “An antenna device and a detecting device having the same,” US20220393366A1, 2022 [Online]. Available: https://patents.google.com/patent/WO2017171407A1/en

[8] I. Y. Shurrab, A. H. El-Hag, K. Assaleh, R. A. Ghunem, and S. Jayaram, “RF-based monitoring and classification of partial discharge on wet silicone rubber surface,” *IEEE Trans. Dielectr. Electr. Insul.*, vol. 20, no. 6, pp. 2188–2194, 2013.